EUROPEAN JOURNAL OF MATERIALS SCIENCE AND ENGINEERING
Volume 10, Issue 4, 2025: 303-326 | www.ejmse.ro | ISSN: 2537-4338

EJMSE

DOI: 10.36868/ejmse.2025.10.04.303

ADVANCED JOINING TECHNIQUES FOR MULTI-MATERIAL STRUCTURES: A REVIEW ON ULTRASONIC CONSOLIDATION, COLD SPRAY, AND ELECTRON BEAM MELTING

Tankiso Lawrence NGAKE[1,*[0000-0002-7397-4581]], Kadephi Vuyolwethu MJALI[1[0000-0002-7848-1647]]

[1] Walter Sisulu University, Department of Mechanical Engineering, PO Box 1421, East London 5200, Eastern Cape, Republic of South Africa

Abstract

The demand for lightweight, high-performance, and multifunctional structures has driven rapid advances in multi-material joining technologies across aerospace, automotive, and electronics industries. Traditional joining methods often struggle with challenges such as thermal distortion, brittle intermetallic formation, and residual stresses when bonding dissimilar materials. This review critically examines three advanced additive manufacturing techniques—Ultrasonic Consolidation (UC), Cold Spray (CS), and Electron Beam Melting (EBM)—that offer promising solutions for multi-material fabrication. The mechanisms, material compatibility, microstructural evolution, and mechanical performance of joints produced by each process are systematically discussed. UC and CS, as solid-state processes, minimize thermal damage and oxidation, enabling strong joints between metals with dissimilar properties. EBM, operating in a high-vacuum environment, allows precise control over microstructure and enables the fabrication of complex, high-performance components. The novelty of this review lies in its integrative comparison of solid-state and fusion-based techniques, with a specific focus on their effectiveness in multi-material structural applications. It emphasizes interface behavior, residual stress development, and scalability challenges, while highlighting underexplored directions such as hybrid processing, interface engineering, tailored material feedstocks, and in-situ monitoring strategies. However, challenges such as bonding efficiency, residual stress management, and scalability remain. Future research directions are proposed, including process optimization, interface engineering, expanded material libraries, and integrated real-time monitoring to fully realize the potential of these emerging technologies for multi-material structural applications.

Keywords: *multi-material joining, ultrasonic consolidation, cold spray, electron beam melting, solid-state bonding, additive manufacturing*

Introduction

With the increasing demand for lightweight, high-strength, and multifunctional materials in the automotive, aerospace, and electronics industries, multi-material joining has become a crucial manufacturing process. Multi-material joining involves integrating different materials—such as metals, polymers, ceramics, and composites—into a single structure to optimize performance while minimizing weight and cost [1].

Traditional joining methods like welding, brazing, and mechanical fastening often face challenges due to differences in thermal expansion, melting points, and mechanical properties between dissimilar materials. Variations in their mechanical, physical, chemical, and thermal properties frequently present challenges when joining dissimilar materials. Differences in elastic modulus between the materials can lead to localized shear stresses under tensile loading, possibly

*Corresponding author: 1tngake@wsu.ac.za

contributing to mechanical failure. Chemical interactions at the interface can form brittle compounds, potentially weakening the joint, especially if these reactions involve volume changes that introduce additional stresses. Furthermore, significant differences in chemical potential between the materials can lead to localized corrosion when exposed to an electrolyte. Another key concern is the mismatch in thermal expansion, which is particularly problematic for brittle materials that must withstand thermal shocks or repeated temperature fluctuations [2-5]. Advanced techniques such as friction stir welding (FSW), adhesive bonding, ultrasonic welding, and hybrid joining methods (e.g., combining mechanical fastening with adhesives) have been developed to overcome these challenges.

This paper reviews three different joining techniques (ultrasonic consolidation, solid-state cold spray, and electron beam melting) to examine the durability and integrity of joints, the compatibility of these techniques with specific materials, and the evolution of microstructural and mechanical properties of joints in dissimilar materials. Ultrasonic Consolidation (UC) is a solid-state additive manufacturing (AM) technique that combines ultrasonic welding with layer-by-layer material deposition to fabricate metallic structures [6]. It was first developed and patented in the early 2000s by Solidica Inc., USA [7] to bond thin metal foils without melting, making it suitable for joining dissimilar metals and embedding secondary materials like fibers or electronics.

In UC, high-frequency ultrasonic vibrations are applied to metal foils under moderate pressure, breaking up surface oxides and allowing atomic diffusion at the interface. This produces a strong metallurgical bond while maintaining the material's original microstructure. Since the process operates at relatively low temperatures (typically below 50% of the melting point), it minimizes residual stresses, distortion, and unwanted phase transformations, which are common in traditional fusion-based processes.

UC is widely used in aerospace, electronics, and energy applications to fabricate lightweight, multi-material components, integrate sensors, and produce functionally graded materials. Research continues to enhance bonding efficiency, material compatibility, and mechanical properties to expand its industrial adoption. A recent study by Behvar et al. [8] indicated a significant grain refinement and higher hardness near the aluminum/copper interface.

Cold spray (CS) is a solid-state deposition process that applies metallic or composite coatings by accelerating fine powder particles to high velocities (300–1200 m/s) using a supersonic gas stream, typically nitrogen or helium [9]. Unlike thermal spray processes, CS does not rely on melting; bonding occurs through severe plastic deformation when particles impact a substrate at high speeds.

Developed in the 1980s in the former Soviet Union, CS has gained significant interest for its ability to deposit coatings with minimal thermal effects, preserving the original microstructure of both the coating and substrate [10]. This makes it ideal for repairing components, fabricating corrosion-resistant layers, and joining dissimilar materials without thermal distortion or phase changes.

CS is widely used in aerospace, defense, automotive, and biomedical industries for component restoration, wear-resistant coatings, and conductive pathways in electronics. Ongoing research focuses on optimizing deposition parameters, expanding material compatibility, and improving adhesion strength for structural applications. Achieving good adhesion and bonding between the deposited material and substrate remains the biggest challenge in CS AM [11]; therefore, this review addresses this challenge by identifying and discussing material suitability and compatibility. Kindermann et al. [12] explore the advancements in CS AM using 3D-printed polymer molds to enhance the fabrication of complex metal parts, which is underexplored. Poor selection of parameters can lead to unwanted tensile stresses; however, techniques such as post-spray heat treatment and laser peening are used to mitigate the challenge [13]. A recent study by Li et al. [14] explores hybrid CS AM techniques for the autonomous repair of complex

geometrical defects in structural components. The study integrates CS technology with defect modelling and precision machining for enhanced repair efficiency.

EBM is an AM technique that uses a high-energy electron beam to melt metal powder layers and build complex components selectively. Developed in the 1990s, EBM is well-suited for processing high-performance metals such as titanium and nickel-based superalloys [15].

The process occurs in a vacuum chamber, preventing oxidation and contamination while enabling high-quality metallurgical bonding. The electron beam provides precise and efficient energy input, resulting in fully dense parts with minimal residual stresses. Compared to laser-based AM processes, EBM typically produces coarser microstructures with excellent mechanical properties and fatigue resistance [16]. However, challenges such as a lack of geometrical accuracy due to the large beam size and a lack of appropriate data processing software for producing 3D multimaterial structures have been identified in [17]. Therefore, this review looks to identify the process limitations and propose future directions.

EBM is widely used in aerospace, medical implants, and high-temperature applications due to its ability to manufacture intricate, lightweight, and structurally optimized components. Current research focuses on improving surface finish, process speed, and expanding material compatibility for broader industrial adoption. For instance, Burkhardt et al.[18] studied the influence of alloy composition on the microstructural and mechanical properties of lattice structures made from high-alloyed austenitic steel produced by selective electron beam melting.

The choice of a joining method depends on factors such as joint strength, thermal effects, corrosion resistance, and manufacturability. Ongoing research focuses on improving the durability of joints, minimizing defects, and enhancing the compatibility of dissimilar materials through surface modifications and interlayer materials. Traditional welding processes, such as arc welding and laser welding, often introduce significant thermal distortions, residual stresses, and metallurgical changes that can compromise the mechanical integrity of structural components. In contrast, advanced joining techniques like UC, CS, and EBM offer several advantages that make them promising alternatives. UC is a low-temperature, solid-state process that minimizes thermal damage and enables the integration of dissimilar materials. CS, another solid-state method, allows for high deposition efficiency with minimal oxidation and retains the original material properties without inducing a heat-affected zone. EBM, a powder-based AM technique, provides precise control over microstructure and mechanical properties while enabling complex geometries that are difficult to achieve with conventional methods. Despite these advantages, a comprehensive evaluation of these techniques in structural applications remains limited, particularly concerning their long-term performance, residual stress development, and joint integrity under service conditions. This review addresses this gap by critically analyzing the capabilities, limitations, and potential of these emerging joining processes for structural design.

This review provides a comparative and integrative analysis of three advanced joining techniques, Ultrasonic Consolidation (UC), Cold Spray (CS), and Electron Beam Melting (EBM), specifically in the context of multi-material structural applications. Unlike existing reviews that focus on single processes or general additive manufacturing, this work bridges solid-state and fusion-based processes by highlighting how their different bonding mechanisms influence microstructural evolution, residual stress formation, and long-term mechanical performance in dissimilar material joints. Moreover, the review emphasizes material compatibility and interface behavior, introduces underexplored research directions, including hybrid processing, interlayer engineering, multi-material feedstocks, and real-time monitoring strategies, which are not comprehensively discussed in prior literature and fills a gap in structural design considerations, by not only reporting process mechanisms and outcomes but also critically assessing scalability, durability, and service-condition performance of multi-material joints.

Multi-material joining techniques

Ultrasonic consolidation

As mentioned in the introduction, UC is a solid-state manufacturing process that utilizes high-frequency ultrasonic vibrations (typically between 20–30 kHz) to bond thin metal foils layer by layer. During UC, a transducer converts a high-frequency electrical signal from the power supply into mechanical vibrations. These vibrations, also known as ultrasonic oscillations, are transferred to the workpiece through a sonotrode (see Figure 1) [19].

The combination of ultrasonic oscillations and the compressive normal force exerted by the sonotrode breaks down surface oxide layers and facilitates atomic diffusion, leading to direct metallic bonding between layers. The bonding mechanism primarily relies on plastic deformation and interfacial diffusion. The ultrasonic oscillations generate dynamic shear stress at the interface between the two workpieces. Due to localized plastic deformation and frictional heat at the contact surface, joint formation occurs at the interface.

The UC system has three key control parameters: oscillation amplitude, which determines how much ultrasonic energy is delivered to the interface; contact pressure, which helps maintain intimate contact between the materials, allowing friction and atomic diffusion to occur; and welding speed.

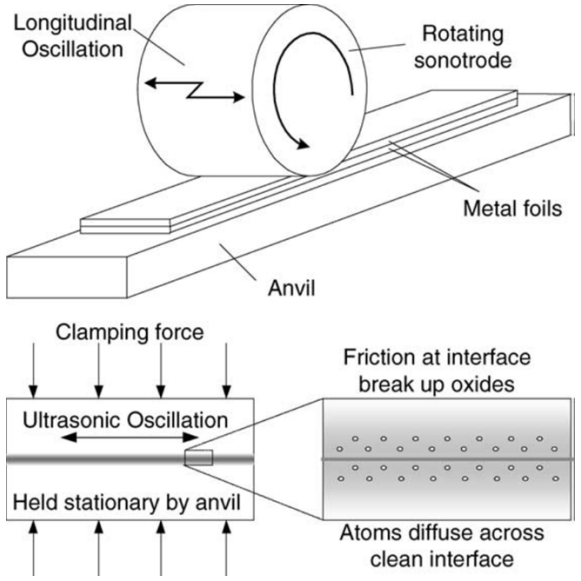

Fig. 1. Schematic diagram of the Ultrasonic Consolidation process [19]

Solid-state cold spray

Cold spraying is a relatively new solid-state coating technique based on supersonic fluid dynamics and high-speed impact dynamics. Initially introduced as a surface coating technology, CS has evolved into a versatile process capable of fabricating full-scale components and repairing critical parts in the aerospace, defence, biomedical, and electronics industries. Recently, CS has been added into the current AM process families, as defined by the "Standard Terminology for Additive Manufacturing Technologies," which is part of the ASTM F2792-12A standard series [20].

The fundamental mechanism of the CS process involves accelerating metal or composite powder particles to high velocities using a heated, pressurized gas stream. The particles, typically within the size range of 10 to 100 μm, are introduced into the gas stream and propelled through a specially designed supersonic nozzle, commonly known as a de-Laval nozzle. The gas, often

nitrogen, helium, or compressed air, is moderately heated to enhance particle velocity without reaching the melting point of the feedstock material [21]. Figure 2 illustrates a typical CS system [22].

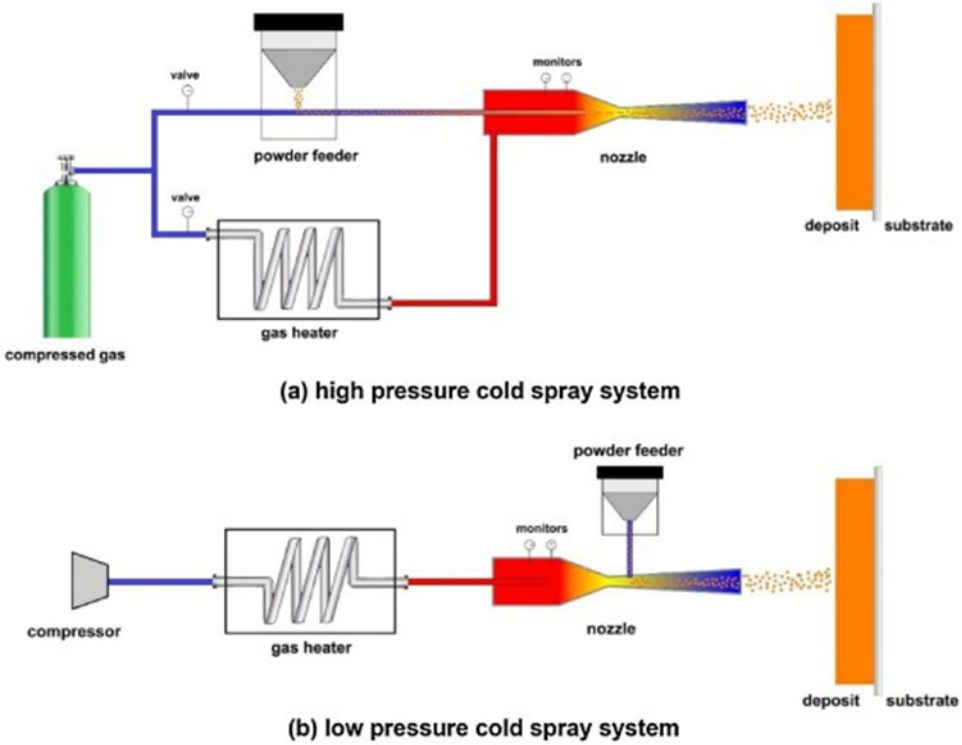

Fig. 2. Schematic of high-pressure and low-pressure cold spray systems [22]

Upon impacting the substrate at speeds ranging from 300 to 1200 m/s, the particles experience intense plastic deformation. Bonding occurs at the impact site if the particle velocity meets or exceeds a material-specific critical velocity. This bonding results from both mechanical interlocking and metallurgical adhesion, forming a dense, well-adhered deposit without any phase transformation or oxidation. Successful deposition in CS depends heavily on the particle impact velocity. Each material has a critical velocity threshold that must be reached for effective bonding. Factors influencing this threshold include particle size, temperature, material ductility, and surface conditions. Typically, gas-atomized spherical powders are used to ensure consistent flow and acceleration. Particles that are too small (<10 μm) or too large (>100 μm) generally fail to achieve adequate velocity and thus do not deposit effectively [22, 23].

A widely accepted theory explaining the bonding mechanism in CS is the concept of Adiabatic Shear Instability (ASI). Proposed by Assadi et al. [24], this theory suggests that during high-velocity impact, the kinetic energy of the particles is rapidly converted into heat. Due to the extremely short interaction time, the heat cannot dissipate, leading to localized thermal softening of the material. If the thermal softening surpasses the concurrent work hardening, a plastic flow forms at the interface, often accompanied by microjetting, which further enhances the bonding quality. For metal-to-metal bonding to occur, the jet has to disrupt the surface oxide layer surrounding the particle and on the substrate surface, which leads to the breakdown or removal of oxides at the surface, as indicated in Figure 3 [25].

CS systems are generally categorized based on gas pressure into high-pressure and low-pressure systems, as depicted in Figure 2. High-pressure systems operate above 1 MPa and utilize industrial-scale heaters and compressors to achieve superior particle velocities, resulting in high

deposition efficiency and strong bonding, making them suitable for structural applications and harder materials. In contrast, low-pressure systems operate below 1 MPa, often using portable compressors and simpler hardware, making them cost-effective and ideal for softer, more ductile materials like aluminum and copper, especially in field repairs. In both configurations, the system design typically includes two gas streams: one that is heated and used for particle acceleration (propulsive gas) and another that carries the powder feedstock (carrier gas). These streams mix before entering the de-Laval nozzle, where the gas expands, accelerating the particles toward the substrate [25].

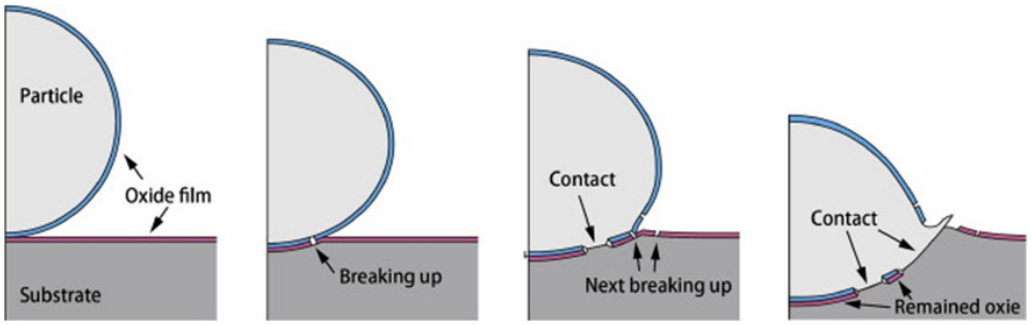

Fig. 3. Deformation of particle upon impact, and break-up of oxide films [25]

Electron beam melting

EBM is an advanced powder bed fusion AM process that utilizes a high-energy electron beam to selectively melt metal powders layer by layer according to a 3D CAD model [26]. Figure 4 illustrates a schematic of an EBM machine. The process begins with a heated tungsten filament generating electrons, which are then collimated and accelerated to approximately 60 keV of kinetic energy. Two magnetic coils guide the electron beam—the first acts as a magnetic lens to focus the beam to a precise diameter (as small as 0.1 mm), while the second deflects it to specific points on the build platform. Since the electron beam gun remains stationary, no mechanical movement is required for beam control. The beam current is adjustable between 1 and 50 mA.

A raking system deposits metal powder in layers typically 0.05–0.2 mm thick in the lower chamber. A computer directs the electron beam to scan the powder bed in a predetermined pattern, selectively melting and fusing the powder into solid metal. This layering process repeats until the part is fully formed. Initially, the beam preheats the powder at high speeds (10^4 mm/s), then switches to a slower scan rate (10^3 mm/s) for melting.

The entire operation occurs in a high-vacuum environment, with residual gas pressures of 10^{-3} Pa in the chamber and 10^{-5} Pa in the electron gun. To prevent electrostatic charge buildup, a small amount of helium gas (10^{-1} Pa) is introduced during melting. After fabrication, the part cools inside the helium-filled chamber to accelerate solidification. Upon removal, the component is encased in loosely sintered powder, which can be easily broken down, sieved, and reused, minimizing material waste. The low oxygen absorption during recycling ensures powder quality is maintained for subsequent builds [27,28].

While single-material builds are straightforward, multi-material fabrication in EBM presents challenges due to material-specific thermal requirements, contamination risks, and limited mid-build access. Nevertheless, successful strategies, such as using machined mask plates and sequential builds, have enabled the fabrication of multi-material parts like Ti–6Al–4V/Cu composites, which exhibit sound bonding and localized hardness enhancements near interfaces.

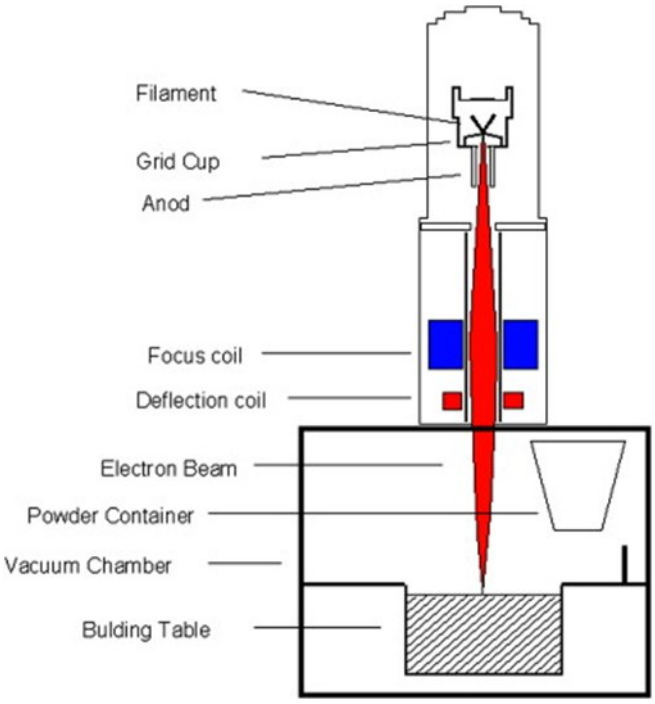

Fig. 4. Schematic drawing of an Arcam EBM machine [28]

A five-step method was developed by Terrazas et al.[29] to fabricate Ti–6Al–4V/copper multi-material components using the Arcam A2 EBM system in separate build runs. First, Ti–6Al–4V bottom halves were fabricated and cleaned, then thoroughly cleaning the system to switch materials. Next, a copper mask plate was CNC-machined to hold the Ti–6Al–4V parts, which were then press-fit into the plate and aligned inside the build chamber. Copper was subsequently deposited atop the titanium inserts in a second EBM run. Finally, the finished multi-material parts were cleaned and extracted, completing the process.

Material suitability and compatibility

Ultrasonic consolidation

The UC works best with materials with good plasticity and high acoustic transmission. The ideal properties for a successful UC are high ductility, moderate hardness, good thermal and electrical conductivity, and acoustic transmission capability. High ductility allows for surface deformation, which enhances bond formation. Materials that are too hard, like AR steel, prevent bonding, while materials that are too soft (such as Lead) may deform excessively. Good thermal and electrical conductivity helps in the even distribution of ultrasonic energy. The materials in UC should efficiently propagate ultrasonic energy for effective bonding.

The most commonly used materials include aluminium alloys because of their high ductility, low melting point, and excellent conductivity [30]. Aluminium alloys such as Al 3003 contain a tenacious oxide layer. Therefore, no preparation is required before welding since UC breaks up and disperses the oxide/contaminants to form atomic bonds [19]. Titanium and Titanium alloys are other common materials used in UC because of their strength, lightweight, and good ultrasonic weldability [31]. Moreover, copper (Cu) and copper alloys possess excellent thermal and electrical conductivity that can be used in UC, especially for heat exchangers and electronics [32]. Nickel (Ni) and nickel alloys can be used in UC, and they are favorites for their good

corrosion resistance and high-temperature performance [33]. Other materials that work well in UC include metal-based amorphous alloys. Wang et al.[34] used iron-based amorphous alloys due to their excellent mechanical properties and corrosion resistance. However, amorphous alloys possess low plasticity and limited size, which inhibits the application of these alloys. UC can bond different metals (such as Al-Cu and Al-Ti) to avoid fusion-related issues like intermetallic formation. The next section will focus on the UC of dissimilar materials. The discussion will be based on the microstructural evolution, mechanical properties, and effects of processing parameters on the quality of joints.

Cold Spray

CS operates below the melting point of materials, and therefore the material suitability depends largely on mechanical properties and thermophysical characteristics rather than melting behaviour. Several material properties play a critical role in determining suitability for CS applications. The most commonly used materials and their properties are summarized in Table 1. Ductility is essential, as ductile materials can plastically deform upon high-velocity impact, forming strong metallurgical bonds without fracturing. Hardness also influences deposition; softer powders are more easily deformed and thus adhere better to the substrate, while very hard materials may resist deformation and potentially erode the substrate surface. Particle size and morphology affect spray efficiency; spherical particles in the range of 10–100 μm with good flowability enhance deposition rates and coating uniformity. Particles with diameters greater than 100 μm or lower than 10 μm are difficult to accelerate with the propulsive gas and thus usually fail to deposit [35]. Thermal conductivity governs how heat is dissipated during impact and contributes to thermal mismatch considerations between the powder and the substrate. Oxidation behaviour is another key factor; materials prone to oxidation can develop surface oxides that impede bonding unless appropriate de-oxidation or surface treatments are applied. Finally, phase stability under high-strain-rate deformation is crucial, as the material must maintain its structural integrity during the CS process to ensure effective bonding and coating performance.

Table 1. Materials commonly used in CS and their suitability properties

Material	Reasons for Suitability
Aluminum (Al) and alloys (e.g., 2024, 7075, 5083)	Lightweight, highly ductile, corrosion-resistant, excellent for structural and repair coatings.
Copper (Cu)	Excellent thermal/electrical conductivity, ductile, often used in electronics or heat exchanger repair.
Titanium (Ti) and alloys	Biocompatible, corrosion-resistant, good strength-to-weight ratio (requires higher velocities).
Nickel (Ni) and alloys (e.g., Inconel)	Oxidation and corrosion-resistant, often used in aerospace and power generation.
Zinc and Zn alloys	Sacrificial coatings for corrosion protection of steel structures.
Tantalum, Niobium	Biocompatible, high corrosion resistance, suitable for biomedical and nuclear applications.

Compatibility between the substrate and powder is crucial when evaluating material suitability for solid-state CS to ensure effective bonding and coating performance. A significant mismatch in the coefficient of thermal expansion (CTE) between the two materials can introduce residual stresses or lead to delamination during thermal cycling. Chemical affinity also plays an important role; minimal oxide formation at the interface enhances bonding, as oxides can act as barriers to adhesion. The hardness of the substrate is another key factor; softer substrates generally facilitate better particle anchoring, whereas harder substrates may require surface preparation, such as grit blasting, to promote adhesion. Moreover, in cases where dissimilar materials are used for the coating and substrate, the bonding behavior, and consequently the adhesion strength, is primarily influenced by differences in key properties, particularly hardness

and density. Generally, a closer match in these properties leads to improved bonding. When the substrate is softer and less dense than the incoming particles, the particles are more likely to penetrate deeper into the surface. This allows the kinetic energy to be distributed over a longer duration and across a larger substrate volume, enhancing the bonding effectiveness [24]. Additionally, mechanical interlocking contributes to bond strength, with rougher substrate surfaces providing improved mechanical grip and improving the overall integrity of the coating.

EBM

Materials suitable for EBM are primarily high-performance metals and alloys that benefit from processing in a vacuum and high-temperature environment. These include titanium and its alloys (such as Ti–6Al–4V, Ti–48Al–2Cr–2Nb), nickel-based superalloys (such as Inconel 625 and 718), cobalt-based alloys (such as Stellite 21), stainless and tool steels (like 17-4 PH and H13), intermetallics (such as γ-TiAl), and to a more limited extent, copper and its alloys. These materials are chosen for their high melting points, excellent mechanical properties, corrosion and oxidation resistance, and, in some cases, biocompatibility. Titanium and intermetallics, in particular, benefit from the vacuum environment of EBM which prevents contamination from oxygen and nitrogen. Using spherical, gas-atomized powders with good flowability also supports consistent layer deposition. Additionally, EBM enables precise microstructural control through thermal management, which is essential for optimizing the performance of aerospace and biomedical components. The process is especially well-suited for reactive and oxygen-sensitive metals that require clean, controlled environments and benefit from the minimal residual stresses generated by the high build temperatures used in EBM. The materials and properties that make them suitable for EBM are summarized in Table 2.

Table 2. Materials commonly used in EBM and their suitability properties

Material	Properties
1. Titanium and Titanium Alloys (e.g., Ti–6Al–4V, Ti–48Al–2Cr–2Nb)	□ High melting point □ Excellent strength-to-weight ratio □ Biocompatibility (ideal for medical implants) □ High affinity for oxygen and nitrogen—thus benefit from EBM's vacuum environment which minimizes contamination □ Good recyclability of unused powder with minimal degradation
2. Nickel-Based Superalloys (e.g., Inconel 625, Inconel 718)	□ High-temperature strength and corrosion resistance □ Excellent fatigue and creep resistance □ Stable microstructure under thermal cycling
3. Cobalt-Based Alloys (e.g., Stellite 21)	□ Wear resistance □ Corrosion and oxidation resistance □ High strength at elevated temperatures
4. Stainless and Tool Steels (e.g., 17-4 PH, H13)	□ Good mechanical properties □ High hardness and wear resistance □ Process stability in vacuum
5. Intermetallics (e.g., γ-TiAl)	□ Lightweight with high-temperature strength □ Suited for aerospace applications □ Require a controlled atmosphere to prevent embrittlement from oxygen pickup
6. Copper and Its Alloys	□ High thermal and electrical conductivity □ Challenges include high reflectivity and conductivity, but EBM's high energy density can overcome these

Microstructural evolution and mechanical properties of multi-material joints

Ultrasonic consolidation

Al-Ti. Several researchers have demonstrated good bonding at the interface of aluminum (Al) and titanium (Ti) composites, indicating strong material compatibility [26-40]. Obielodan et al. [36] showed that embedding materials such as boron powder can enhance the Al/Ti bonding

interface, as illustrated in Figure 5. The embedded boron powder alters the local composition, enabling localized property control within the structure and facilitating the fabrication of particle-reinforced composite materials. A well-bonded Al/Ti interface is achieved when aluminum and titanium foils undergo plastic flow around the embedded boron particles, ensuring a strong metallurgical connection (see Figure 5).

Different aluminum and titanium alloys initially possess distinct microstructures before undergoing UC treatment. Understanding the original microstructure is crucial for assessing the impact of UC on the bonded zone. Sridharan et al. [37] investigated the microstructural and textural evolution in Al/Ti dissimilar welds. Using Al-6061-T6 as a substrate and bilayers of Al-1100 and commercially pure titanium (CP-Ti), they observed no intermetallic formation during bond formation. Additionally, they reported a decrease in the grain size of Al-1100, while the grain size of CP-Ti remained unchanged after processing.

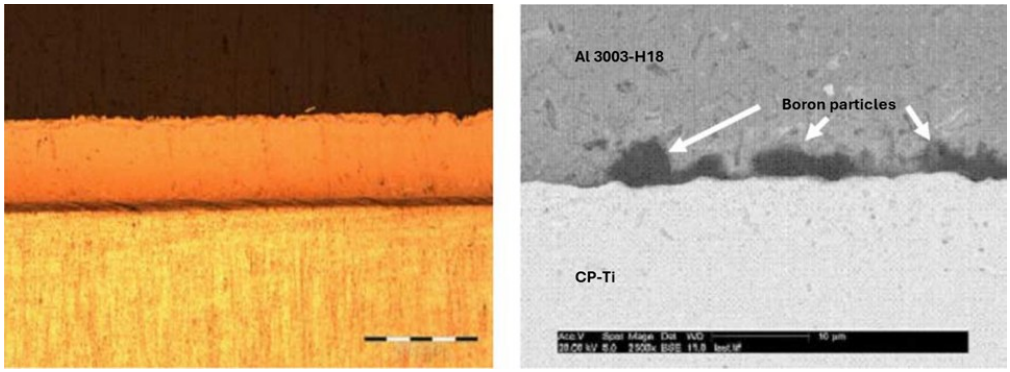

Fig. 5. (left) Titanium/Al 3003 with elemental boron powder at the interface on Al 3003 substrate & (right) 2500x magnification SEM micrograph of boron powder at the interface between Ti and Al 3003 foils [36]

The Al/Ti interface exhibits several notable microstructural characteristics and transformations. According to Bo et al. [38], UC treatment affects the interface in the following ways:

(i) Grain refinement occurs due to severe microplastic deformation.

(ii) The strip-like grains in the original microstructure break into multiple segments, forming smaller grains.

(iii) Recrystallization occurs due to the high dislocation density accumulated during processing.

Bo et al. [38] also examined the influence of static force and ultrasonic amplitude on interfacial bonding. Their findings indicate that bonding strength initially increases with static force but later decreases beyond a certain threshold. Furthermore, bonding strength improves with increasing amplitude. Zhou et al. [39] investigated the effect of ultrasonic amplitude on microstructural characteristics, bonding quality, and mechanical properties by varying the amplitude from 28 μm to 32 μm. Their findings include:

(i) Both amplitudes produced a well-bonded interface with no defects.

(ii) Higher amplitudes led to severe plastic deformation, resulting in grain refinement at the interface.

(iii) Samples processed at lower amplitudes exhibited higher yield strength (YS), ultimate tensile strength (UTS), and flexural strength (FS) compared to those processed at higher amplitudes.

(iv) The Ti layer's Hardness and near-interface zone hardening decreased at higher amplitudes.

The in-situ tensile behavior of Ti/Al laminated composites was studied by Cheng et al. [40], and the resulting tensile stress-strain curves are shown in Figure 6. As observed in Figure 6, Al/Al sheet materials exhibit lower strength and plasticity due to retained rolling deformation, which limits their deformation capacity. Ti foil demonstrates the highest strength with intermediate ductility, while the strength of Ti/Al composites falls between that of Ti and Al.

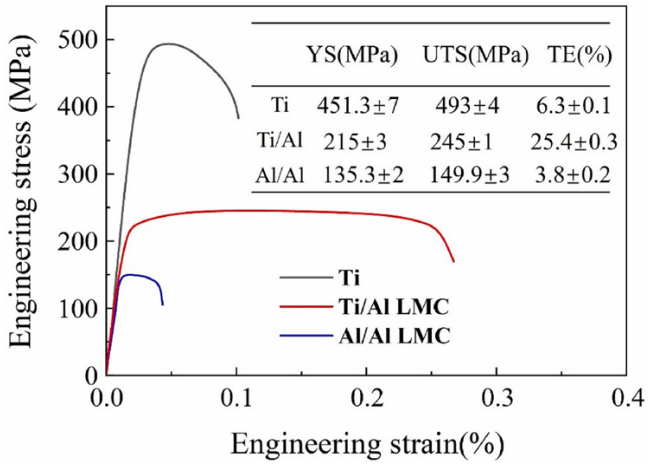

Fig. 6. Tensile engineering stress-strain curves of Ti/Al, Al/Al and Ti materials [40]

Al-Cu. Commercially pure aluminum foils offer several advantages, including high purity, excellent plasticity, good compressive strength, ease of shear processing, suitable ductility, and cost-effectiveness. In comparison, pure copper foils exhibit superior ductility and exceptional thermal and electrical conductivity and can be alloyed in various ways. Using UC to fabricate Al/Cu laminated composites helps prevent the formation of new interfacial phases during processing due to the low temperatures involved. This technique also allows both aluminum and copper foils to fully retain and utilize their inherent plasticity and ductility [41, 42].

Numerous researchers have investigated the bond formation and microstructural evolution of Al/Cu composites during UC welding. Fujii et al. [43] reported that compressive deformation combined with ultrasonic sliding at the weld interface promotes mechanical mixing and aluminum alloy flow, leading to the oxide layer's disruption and dispersion, as shown in Figure 7. The dispersion of the oxide layer facilitates direct contact between newly exposed aluminum and copper surfaces, enabling extensive metallurgical bonding across the interface.

Sriraman et al. [32] suggested that bonding between Al and Cu occurs through dynamic recrystallization and the potential migration of grain boundaries across the interface. They also observed a reduction in grain size near the interface compared to the original foil grain size. The resulting finer-grain structure contains a higher fraction of high-angle grain boundaries, further supporting the occurrence of recrystallization. Additionally, a gradual decrease in average grain size towards the interface contributes to increased hardness in this region [8].

Deformation at the Al/Cu interface leads to the formation of a recrystallized microstructure characterized by a {111}<011> or {001}<100> shear texture. Furthermore, Fujii et al. [43] observed the formation of Al_2Cu intermetallic compound layers along the weld interface (see Figure 8), which were not present in the findings of [44]. These intermetallic layers grow progressively with welding time, developing into uniform structures with increasing thickness, as illustrated in Figure 8.

According to [32], hardness decreases from the aluminum foil towards the interface. In contrast, [44] reported a slight increase in hardness in this region, attributed to grain refinement.

Additionally, the tensile strength of Al/Cu composites improves significantly after UC welding due to grain refinement, increased dislocation density, and enhanced material strength [44]. However, despite the improvement in strength, the plasticity of the pure aluminum and copper foils decreases. This reduction is attributed to the formation of micro-cracks, which result from increased surface roughness of the base material during welding caused by the downward pressure of the welding head.

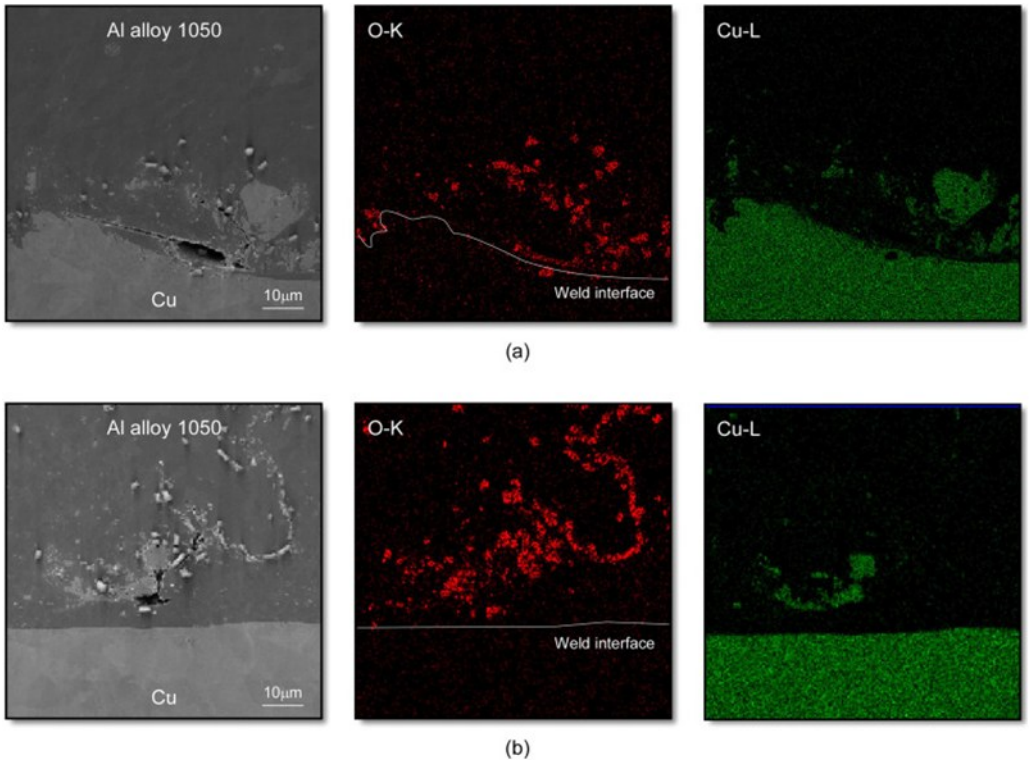

Fig. 7. SEM images taken near the weld interfaces of samples welded for (a) 0.2 s and (b) 0.4 s [43]

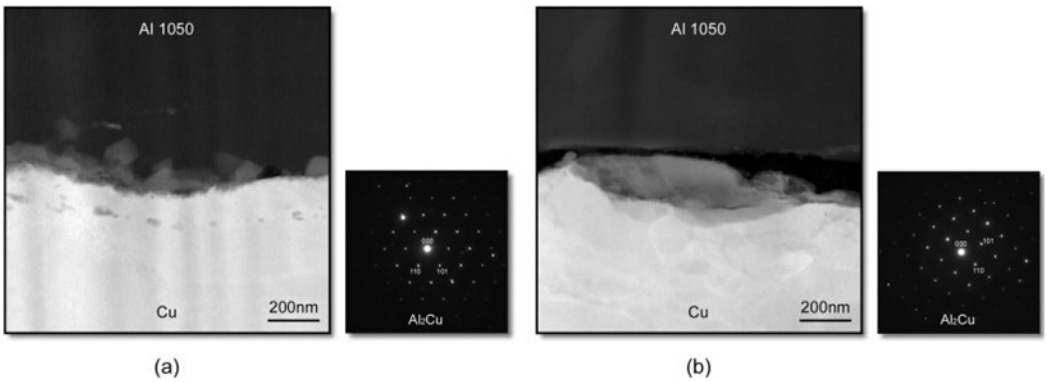

Fig. 8. Annular dark field STEM images taken around the weld interfaces between Al alloy 1050 and Cu in (a) 0.2 s and (b) 0.4 s samples, and selected area diffraction patterns obtained [43]

Al-Ni. There are limited studies on the UC of aluminum and nickel dissimilar materials. Dezhi Li indicated more power is required to bond harder materials such as Ni during UC due to less plastic deformation at the interface [30]. However, Yang et al. [45] and Ram et al. [46] showed a good bonding between aluminum and nickel. They further demonstrated that the bond formation is not brought about by mechanical interlocking, localized metal melting, diffusion, or recrystallization but rather due to atomic-level forces across the nascent metal contact points. Furthermore, UC appears to involve a recurring cycle of contact and bonding phases, each triggering the next. In the contact phase, plastic deformation of existing bonds creates new contact points. In the subsequent bonding phase, oxide layers are eliminated, allowing metallurgical bonds to form at the newly established contact points. Neither of the studies investigated the mechanical properties of the Al-Ni weld joints. Erdeniz et al. [47] fabricated Al-Ni energetic composites using ultrasonic powder consolidation. Their results show that a densification of Al-Ni powders reached 95-100% of theoretical density above a temperature of 523 K. Moreover, the microstructure showed well-distributed Ni particles in a fully densified Al matrix with no discernible prior-particle boundaries.

Cold Spray

Cu-Al. Bonding between aluminum and copper follows deformation-driven oxide disruption for successful bonding (discussed in section 2.2). Hussain et al. [48] emphasize the asymmetry in bond formation when aluminum is sprayed on copper versus copper on aluminum. They found that copper-on-aluminum leads to better metallurgical bonding due to greater substrate deformation and oxide layer disruption at the interface. Copper on aluminum showed 46% intermetallic coverage, while aluminum on copper showed only 13%. In another study by Hussain et al. [49], substrate surface preparation significantly influenced bond quality. Polished and annealed aluminum substrates promoted more effective metallurgical bonding, while grit-blasting reduced bond strength due to work-hardening effects that limited deformation during impact. King et al. [50] combined experimental and FEM simulations to show that bonding improves with increasing gas temperature, particularly when copper is sprayed onto softer substrates like commercial-purity aluminum. The formation of a thin molten interfacial layer, especially at higher temperatures, was also noted, indicating that localized melting may assist in metallurgical bonding, even in a nominally solid-state process. The bond strength correlates with metallurgical bonding quality and substrate preparation. The pull-off tests by Hussain et al. [49] showed higher bond strength for polished and annealed substrates due to enhanced oxide disruption and clean bonding interfaces. The lowest bond strengths were associated with grit-blasted surfaces.

Furthermore, Hussain et al. [48] noted the asymmetric behavior in the bond strength results, where copper-on-aluminum coatings exhibited stronger adhesion than aluminum-on-copper, reinforcing the importance of substrate hardness and oxide removal mechanisms in achieving robust mechanical properties.

Ni-based superalloys. CS technology has emerged as a promising solid-state deposition technique for nickel-based superalloys due to its ability to produce oxidation-free, dense coatings or components with superior mechanical integrity. A comprehensive review of the solid state CS AM of Ni-based super-alloys was reported on [51]. Luo et al. [52] mechanically blended coarse 410 stainless steel (410SS) particles into the IN718 feedstock to induce a hammering effect during deposition, which greatly enhanced the plastic deformation and inter-particle bonding of IN718. Their findings include:

- Porosity reduction from 5.6% (pure IN718 spray) to 0.26% using 50 vol% micro-forging (MF) particles.
- Ultimate tensile strength improved from 96 MPa to 464 MPa in as-sprayed samples, and up to 1089 MPa after heat treatment at 1200 °C for 6 hours, as indicated in Figure 9.

- Figure 10 illustrates that microstructural refinement was evident, with broken dendritic structures and improved bonding.
- No contamination occurred from MF particles due to their low velocity and limited embedment.

Chaudhuri et al. [53] focused on the microstructural evolution of cold-sprayed Inconel 625 (IN625) coatings on low alloy steel substrates. Figure 11 shows the proposed microstructural evolution mechanism between the Inconel 625 and low alloy steel. During cold spraying, a supersonic stream of nearly spherical IN625 particles impacts a grit-blasted 4130 steel substrate, whose roughened surface aids mechanical interlocking. Upon impact, the substrate surface experiences severe grain refinement due to high-energy particle collisions, and the incoming IN625 particles fragment, forming a fine-grained layer at the interface. As spraying progresses, particles deform plastically into splats under high strain rates. Dislocations accumulate and rearrange into low-energy cell structures, aided by localized adiabatic heating. This evolution results in the formation of low and high-angle grain boundaries within splats. Splat-splat interfaces form under high contact pressure, exhibiting high defect densities and shear bands due to adiabatic shear instability, further contributing to the complex microstructure of the coating. Wong et. al [54] demonstrated that varying gas can change particle velocity, with nitrogen producing higher particle velocity than helium. Moreover, combining high particle velocity during spraying with post-process annealing can significantly enhance mechanical properties and bonding in cold-sprayed IN718 deposits. A good adhesion strength (~57 MPa), low porosity (~0.3%), and dense microstructure were obtained by Wu et al.[55] during cold-spray between IN625 and Al6061 substrate. In comparison, Levasseur et al. [56] addressed the lack of interparticle bonding in CS IN718 coatings, which limits their as-sprayed strength. By applying pressureless sintering at temperatures ranging from 1200°C to 1250°C for up to 180 minutes, they significantly improved densification (up to 99.8%) and enhanced mechanical strength, reaching a flexural strength of 2303 MPa after aging treatment. Higher microhardness was achieved during CS of IN625 compared to bulk IN625 due to grain refinement and work hardening [55]. Silvello et al. [57] extended this investigation to fatigue performance. Using IN625 coatings sprayed at 1000 °C and 50 bar on V-notched carbon steel substrates, they observed improved fatigue resistance and crack propagation resistance.

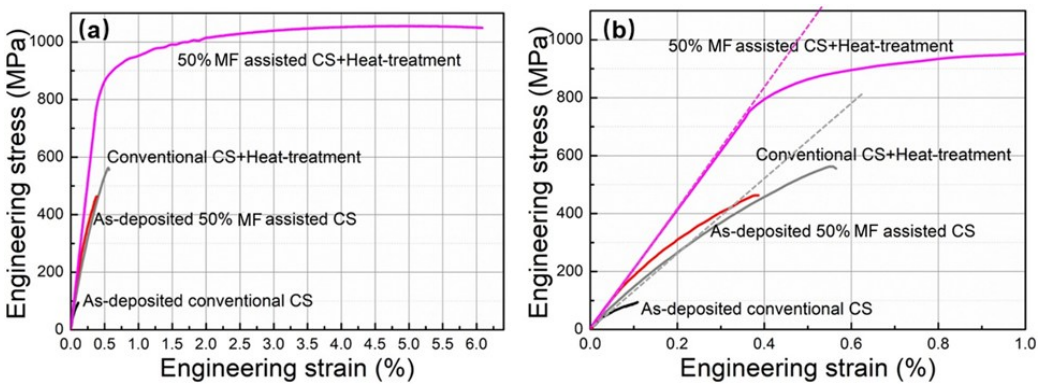

Fig. 9. Tensile curves of the as-deposited and heat-treated IN718 deposit; (b) is a close view of (a) in the strain range of 0 to 1%, showing the nonlinear behaviour of the as-deposited [52].

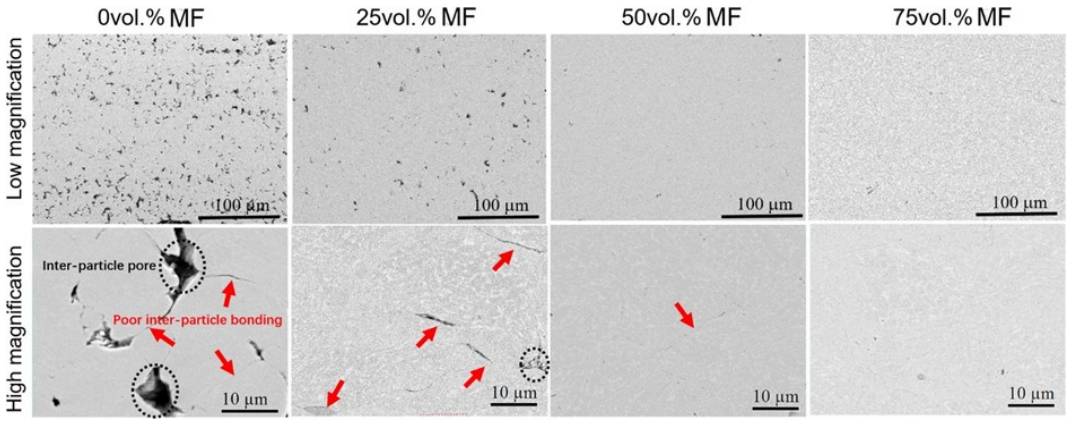

Fig. 10. Cross sectional microstructure of the cold sprayed IN718 deposits as a function of the MF particle content in the mixed spraying powders [52]

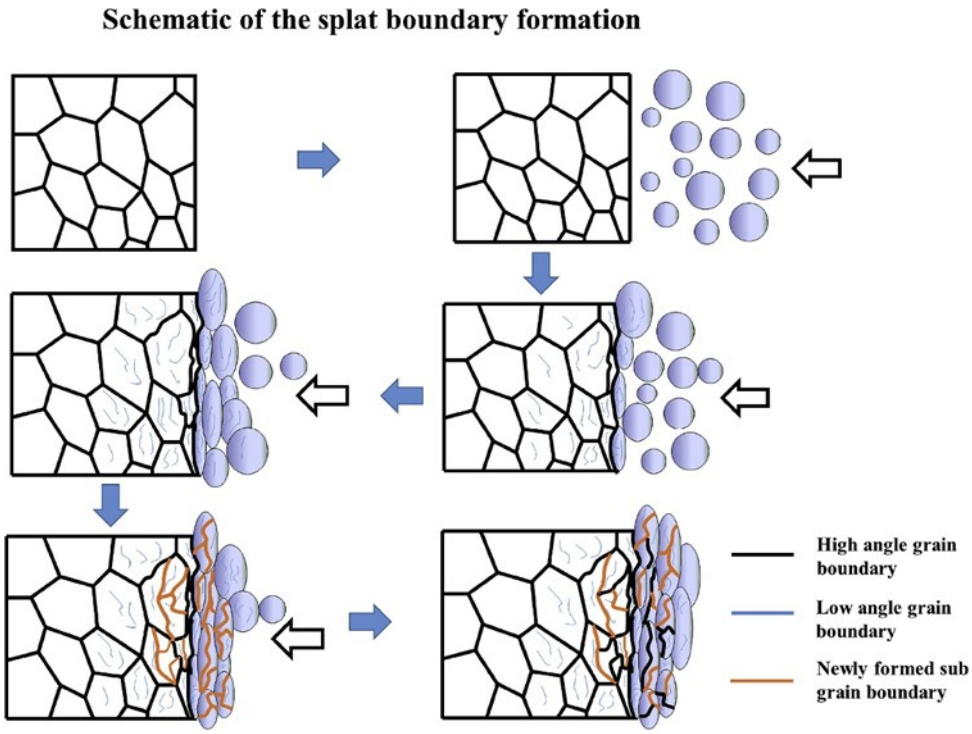

Fig. 11. Proposed steps leading up to the observed coating microstructure within a splat and splat boundary [53]

Ti-based CS. Titanium shows significant promise as a protective coating against corrosion and as a material for near-net-shape production in aerospace applications, where minimizing machining expenses is crucial. However, challenges in cold spraying titanium arise from its elevated critical velocity requirements, strong tendency to oxidize, and unique crystalline structure. The bonding mechanisms in cold-sprayed titanium coatings are primarily governed by high strain-rate plastic deformation and adiabatic shear instability at particle-substrate interfaces. Hussain et al. [58] systematically investigated the impact phenomena of titanium particles on

various ferrous substrates (low carbon steel, Armco iron, and austenitic stainless steel). Their work revealed that:

- Localized substrate deformation dominated when titanium impacted softer Armco iron, with particles embedding into the substrate without significant jetting
- Extensive particle jetting occurred on harder substrates (low carbon steel and stainless steel), promoting bonding through severe plastic deformation
- The Johnson-Cook material model effectively predicted high strain-rate deformation behavior, showing that Armco iron underwent greater plastic strain (0.34) compared to carbon steel (0.23) under similar conditions

Bae et al. [59] expanded on these findings by linking experimental observations with finite element modeling of titanium particle impacts. Their key conclusions included:

- A thermal boost-up zone (TBZ) forms at particle-substrate interfaces due to adiabatic shear instability, which is critical for successful bonding.
- Titanium exhibits relatively low thermal softening sensitivity compared to other metals, requiring higher impact velocities for effective deposition.
- Powder preheating (up to 600°C) enhanced thermal softening and improved coating density by promoting more severe plastic deformation.

Moy et al. [60] demonstrated a heavy particle deformation and penetration (10-30 μm) into the substrate during CS of Ti powder on Al 6063 substrate, as illustrated in Figure 12. Furthermore, they indicated sharp compositional transitions (<5 nm wide) at particle-substrate interfaces, indicating limited interdiffusion. Multiple studies investigated how CS parameters influence coating characteristics. Wang et al. [61] compared nitrogen and compressed air as propellant gases and found out that nitrogen produced denser coatings (5.8% porosity) compared to air (10% porosity) at similar conditions, attributed to reduced titanium oxidation. Additionally, increasing gas pressure from 1.5 to 2.0 MPa decreased porosity from 17.5% to 10.0% in air-sprayed coatings. Gulizia et al. [62] found that the porosity dropped sharply from 11% to 1% when nitrogen pressure increased from 2.0 to 3.0 MPa at 400°C. Very high pressures (>3.0 MPa) could reduce deposition efficiency due to bow shock effects deflecting smaller particles. According to Wong et al. [63], angular powder particles achieved higher velocities than spherical ones at equivalent conditions, leading to better deposition efficiency. Moreover, smaller particles (<25 μm) are deposited more effectively than larger ones due to higher achievable velocities. This indicates the significance of particle shape. An increase in gas/operating temperature results in a decrease in porosity, an increase in particle velocity, and more dense and harder coatings.

EBM. Recent advancements have expanded EBM's capabilities to include the production of multi-material and functionally graded materials (FGMs), which are critical for applications requiring tailored mechanical, thermal, or corrosion-resistant properties. Multi-material fabrication by EBM requires some innovations in hardware and methodologies. Zykova et al. [64] demonstrated the feasibility of producing Ti6Al4V/5%Cu composites using simultaneous feeding of Ti and Cu wires. This approach refined coarse columnar grains into equiaxed ones and introduced dispersion hardening via Ti2Cu precipitates, enhancing tensile strength by 20% (though ductility decreased threefold). Guo et al.[65] developed a vibration-based powder-supplying system for blending Ti6Al4V and Ti47Al2Cr2Nb powders in tailored proportions. Their comb-inclined spreading method reduced stress on powder spreaders, improving reliability. The resulting FGMs exhibited a crack-free interface with a 300 μm transition zone and staircase-like compositional gradients. Hinojos et al. [66] explored EBM for joining Inconel 718 and 316L stainless steel, achieving fine microstructural bonds without filler materials. The process minimized heat-affected zones (HAZ) and reduced thermal distortion compared to traditional welding, though cracking occurred in 316L/IN718 interfaces due to thermal stress, as shown in Figure 13. In Ti6Al4V/Cu composites, Cu addition promoted equiaxed grain formation and Widmanstätten structures with supersaturated Cu in α/β phases. Ti2Cu precipitates contributed to

dispersion hardening [64]. Ti6Al4V/5%Cu showed a 20% increase in ultimate tensile strength but reduced ductility due to grain boundary wetting and solid solution hardening as depicted in Figure 14 [64]. Inconel 718/316L joints exhibited hardness gradients, with the interface region showing lower hardness (135 HV) compared to bulk materials (IN718: 241 HV; 316L: 148 HV) [66].

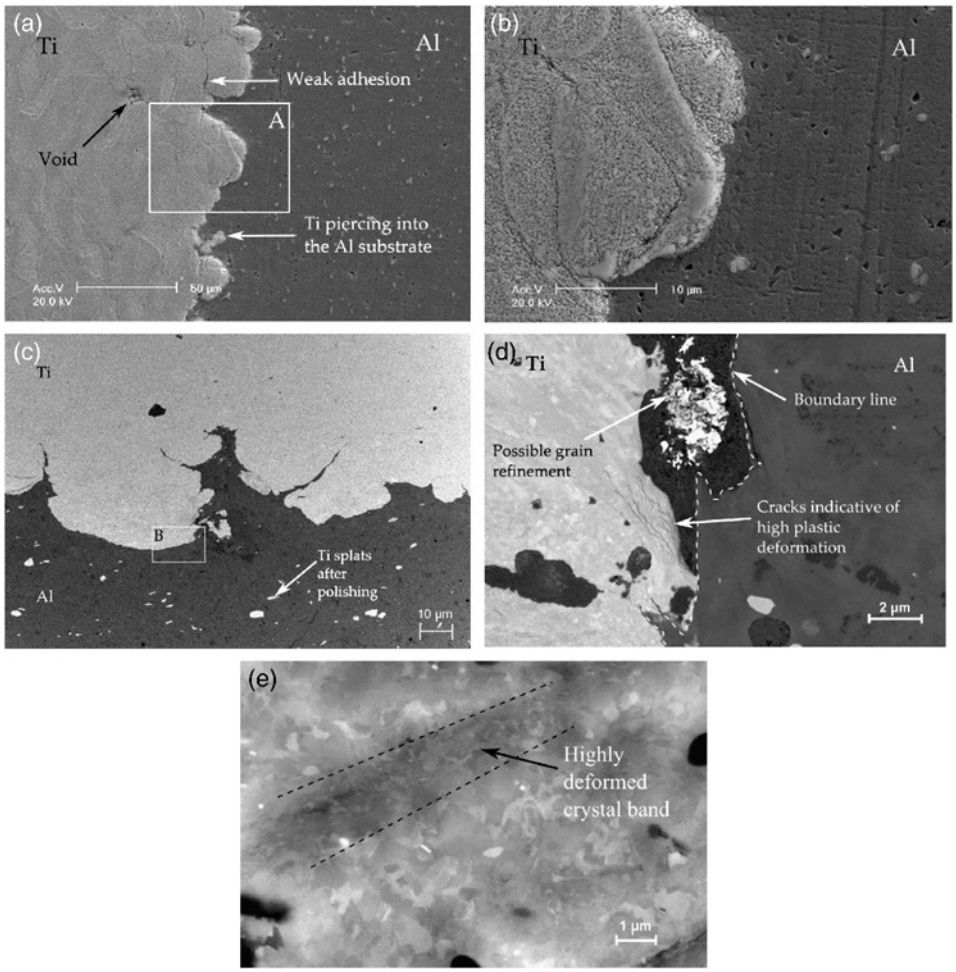

Fig. 12. SEM micrographs of the cold spray Ti interacting with the Al 6063 substrate: (a) imperfection in the coating near the interface; (b) magnification of area A showing a severe deformation of the particles with probable amalgamation of the different particles; (c) interface region finely polished with argon gas; (d) high plastic deformation at the interface but no noticeable fusion between the two materials (region B) – contrasted region may be indicative of grain refinement and; (e) highly deformed crystal structure of the Al 6063 substrate at approximately 0.5 mm from the interface [60]

Zhu et al. [67] explored the fabrication of Ti6Al4V/Cu/316L multi-materials using electron beam freeform fabrication (EBF³), highlighting that direct deposition of 316L on Ti6Al4V led to severe cracking due to brittle Fe–Ti intermetallic compound (IMC) formation. Introducing a copper interlayer effectively suppressed continuous Fe–Ti IMCs, resulting in improved interfacial strength, with the Ti64/Cu interface achieving a maximum micro-hardness of 490 HV and a shear strength of 196.5 MPa. Similarly, Terrazas et al.[29] demonstrated a practical method for multi-material EBM by fabricating Ti–6Al–4V parts, fitting them into a machined copper mask plate, and depositing copper in a second EBM run. Although successful metallurgical

bonding was achieved, manual registration introduced slight misalignments, and hardness values near the interface were higher than in bulk regions.

Meanwhile, Ge Wenjun et al. [68] investigated an alternative approach using blended Ti6Al4V and Ti45Al7Nb powders in EBM, finding that rapid cooling produced a martensitic phase near the substrate and an α2+β phase after reheating, with fabricated components exhibiting high tensile strength (up to 1214 MPa) and good ductility (18% elongation).

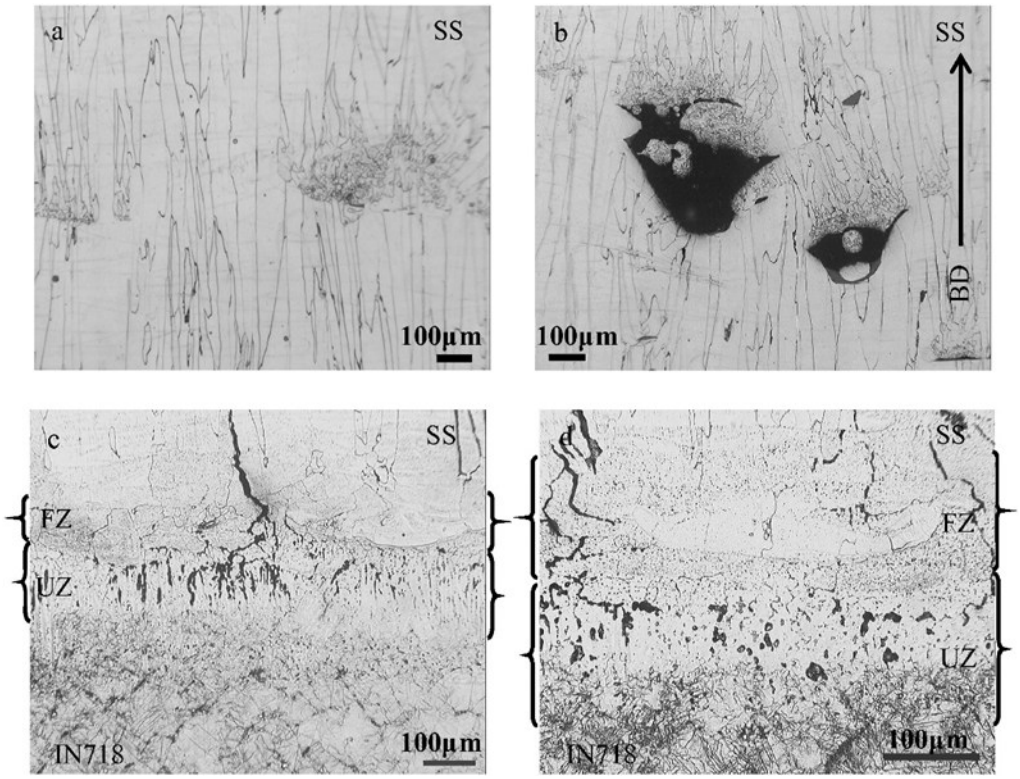

Fig. 13. Micrographs of the fabricated 316L SS. Micrographs (a) and (b) show defects of par-melted and unmelted layers with entrapped powder. Microstructures of the fabricated 316L [66]

Process limitations

Ultrasonic consolidation

UC offers advantages like low-temperature bonding and the ability to embed fibers or sensors; however, it has several process limitations, such as:

- Material Limitations
- Geometric Constraints
- Bonding Quality Issues
- Process Speed & Scalability
- Energy transfer efficiency
- Design complexity limitations
- Equipment & Cost Factors

UC is primarily restricted to soft, ductile metals such as aluminum and copper, while harder or brittle materials are difficult to bond effectively. As more layers are built up, the ultrasonic energy attenuates through the stack, decreasing bond quality and limiting the achievable build height. The surface finish of UC parts tends to be rough, often requiring additional machining to meet dimensional and surface accuracy standards. Weak interfaces and delamination can occur if

parameters like pressure, vibration amplitude, and surface preparation are not carefully optimized. UC also has a relatively slow deposition rate compared to other AM methods, making it less ideal for large-scale production. The process is constrained by the thickness of the metal foils, typically around 100–200 micrometers, which limits the volume build-up speed. Furthermore, efficient energy transfer depends heavily on having clean, oxide-free surfaces, as contamination or surface roughness can significantly hinder bonding. Complex internal features, such as enclosed hollow sections, are challenging to fabricate without integrating additional machining steps. The sonotrode, which delivers the ultrasonic vibrations, is subject to wear over time, especially when processing harder materials, leading to the need for frequent maintenance or replacement.

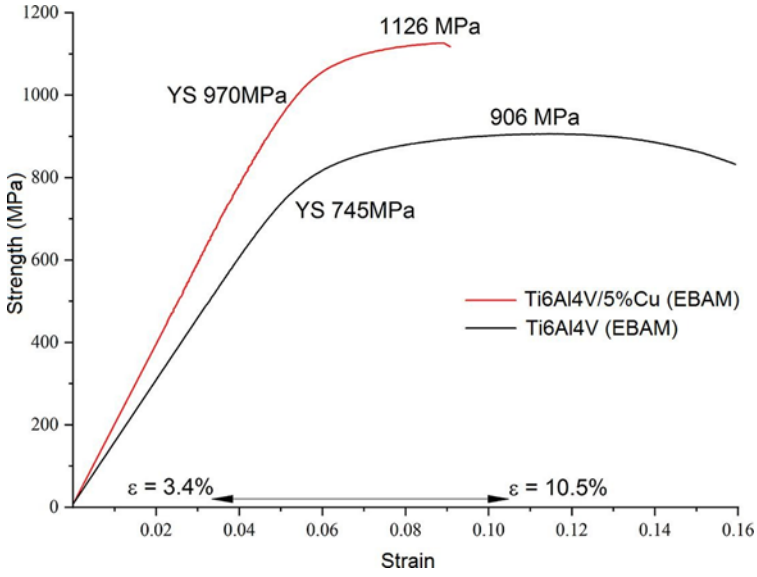

Fig. 14. Stress–strain diagram for Ti6Al4V/5%Cu and Ti6Al4V produced by the EBAM [64]

Cold Spray

In CSAM, metallic particles are accelerated at high velocities (often by a compressed gas) and impact a substrate to create bonding without melting the material. Although it offers advantages like low thermal distortion and the ability to work with oxidation-sensitive materials, there are significant challenges, such as;

- Material Restrictions
- Bonding and Porosity Issues
- Surface Preparation & Substrate Limitations
- Geometric Challenges
- Process Control & Scalability
- Residual Stresses & Distortion
- Equipment & Cost Factors

CS is mainly effective for ductile metals such as aluminum, copper, titanium, and their alloys; brittle or very hard materials are difficult to deposit successfully because they cannot deform plastically enough upon impact. Achieving strong inter-particle bonding also requires very high particle velocities, sometimes limiting the process to expensive high-pressure systems and specific nozzle designs. Surface preparation of the substrate is critical — poor surface conditions can result in weak adhesion and delamination. Moreover, the final parts often have relatively high

porosity and may require post-processing, such as hot isostatic pressing or heat treatment, to improve density and mechanical properties.

The process also struggles with producing very fine features or sharp edges, as the spray tends to deposit material more broadly and less precisely compared to processes like laser-based AM. Additionally, complex internal structures or overhangs are difficult to achieve without using support materials or hybrid manufacturing approaches. Residual stresses can build up during deposition due to the repeated high-energy particle impacts, potentially leading to warping or cracking, especially in thicker builds. Lastly, the equipment and gas consumption (especially for high-pressure helium systems) can be costly, limiting the widespread adoption of CSAM for certain applications.

EBM

EBM requires a high-vacuum environment to prevent electron scattering, which limits the process to materials that are vacuum-compatible and rules out metals that outgas significantly (like zinc or magnesium alloys). The high processing temperatures (often above 700°C) needed to maintain powder bed conductivity can cause unwanted material interactions, phase transformations, and even alloying between different materials during multi-material builds. Controlling the interface between dissimilar materials is especially challenging: differences in melting points, thermal expansion, and diffusion behavior can lead to cracks, delamination, or the formation of brittle intermetallic phases.

Additionally, the EBM process uses a single powder feedstock at a time, so switching between materials requires either complex powder delivery systems or manual intervention, which increases the risk of contamination and prolongs production time. The resolution of EBM is relatively coarse compared to laser-based AM, making it harder to produce fine features or sharp material transitions in multi-material components. Furthermore, EBM can generate significant residual stresses because of the rapid heating and cooling cycles, especially when joining materials with mismatched thermal properties.

Another limitation is the limited material library available: most successful EBM applications today focus on titanium alloys, cobalt-chromium alloys, and a few nickel-based superalloys. Expanding to a broader set of materials, especially dissimilar combinations, remains challenging due to process complexity and limited process parameter control compared to laser-based AM systems. Finally, the EBM system and its maintenance are expensive, and process parameters are often not flexible enough to easily accommodate the different thermal needs of each material in a multi-material build without extensive requalification.

Conclusions and Future Work

This review presented a comprehensive analysis of three advanced multi-material additive manufacturing processes—Ultrasonic Consolidation (UC), Cold Spray (CS), and Electron Beam Melting (EBM)—focusing on their mechanisms, material compatibility, microstructural evolution, mechanical performance, and associated challenges.

UC stands out for its ability to bond dissimilar metals at low temperatures, minimizing thermal distortion and enabling the fabrication of multi-functional structures. However, limitations such as energy attenuation through stacked layers and challenges with harder materials restrict its broader application. As a solid-state process, CS excels in producing dense, oxidation-free coatings and near-net-shape components with minimal thermal impact. Nonetheless, achieving strong metallurgical bonds, especially for harder or less ductile materials, remains challenging, and high equipment costs can hinder large-scale adoption. EBM, operating under vacuum and at elevated temperatures, enables the fabrication of fully dense components with intricate geometries and offers advantages for reactive materials like titanium alloys. Yet, multi-material

fabrication with EBM still faces difficulties, including thermal stress management, limited material combinations, and coarse resolution compared to laser-based methods.

Although each process shows significant promise for multi-material structural applications, further developments are needed to fully harness their potential. Future research should focus on optimizing process parameters, such as pressure, ultrasonic amplitude, particle velocity, and beam current, to improve joint quality and reliability across different material systems. Expanding the range of suitable feedstock materials, including hybrid powders, tailored alloys, and layered composites, will be essential for broadening the industrial applications of UC, CS, and EBM. Additionally, advanced strategies for controlling multi-material interfaces, such as surface engineering, interlayer design, and in-situ alloying, are needed to mitigate interfacial defects and enhance mechanical performance. Investigating the development of residual stresses, long-term fatigue behaviour, and environmental durability of multi-material joints remains critical for certifying these technologies for structural applications. The integration of in-situ monitoring systems, machine learning models, and adaptive control algorithms can further improve process reliability, repeatability, and scalability. Finally, efforts toward improving sustainability, such as recycling feedstocks, reducing energy consumption, and minimizing production costs, will be crucial for enabling the widespread industrial adoption of multi-material AM processes.

Acknowledgments / Funding body

This work was supported by Walter Sisulu University (WSU) Directorate of Research and Innovation (DRS). This research was funded by Walter Sisulu University, Directorate of Research and Innovation under research niche area (RNA) Process Technologies and Material Science in Engineering.

References

[1] R. Sankaranarayanan, N.R.J. Hynes. *Prospects of Joining Multi-Material Structures*. **AIP Conference Proceedings**, **1953**, 2018, 130021.

[2] P. Kaushik, D.K. Dwivedi. *Al-steel dissimilar joining: Challenges and opportunities*. **Materials Today: Proceedings**, **62(12)**, 2022, 6884–6899.

[3] T. Majeed, Y. Mehta, A.N. Siddiquee. *Challenges in joining of unequal thickness materials for aerospace applications: A review*. **Proceedings of the Institution of Mechanical Engineers, Part L: Journal of Materials: Design and Applications**, **235(4)**, 2021, 934–945.

[4] H. Li, X.S. Liu, Y.S. Zhang, M.T. Ma, G.Y. Li, J. Senkara. *Current research and challenges in innovative technology of joining dissimilar materials for electric vehicles*. **Advanced High Strength Steel and Press Hardening (ICHSU2018)**, 2018.

[5] D. Jones, J. Jebaraj, R. Sankaranarayanan. *Joining of dissimilar materials—challenges & possibilities*. **AIP Conference Proceedings**, **2220(1)**, 2020, 140036.

[6] G.D. Janaki Ram, C. Robinson, Y. Yang, B.E. Stucker. *Use of ultrasonic consolidation for fabrication of multi-material structures*. **Rapid Prototyping Journal**, **13(4)**, 2007, 226–235.

[7] D. White. *USA Patent 6519500*. 2003.

[8] A. Behvar, S.I. Shakil, H. Pirgazi, M. Norfolk, M. Haghshenas. *Multi-layer solid-state ultrasonic additive manufacturing of aluminum/copper: local properties and texture*. **International Journal of Advanced Manufacturing Technology**, **132**, 2024, 2061–2075.

[9] A. Papyrin, V. Kosarev, S. Klinkov, A. Alkhimov, V.M. Fomin. *Cold Spray Technology*. **Elsevier**, 2006.

[10] A. Papyrin. *Cold Spray Technology*. **AM&P**, **159(9)**, 2001.

[11] A. Kafle, R. Silwal, B. Koirala, S. Lu, W. Zhu. *Advancements in Cold Spray Additive Manufacturing: A Review of Materials and Processes*. **IISE Annual Conference & Expo**, 2025.

[12] P. Kindermann, M. Strasser, M. Wunderer, I. Uensal, M. Horn, C. Seidel. *Cold spray forming: a novel approach in cold spray additive manufacturing of complex parts using 3D-printed polymer molds*. **Progress in Additive Manufacturing**, **9**, 2024, 1567–1578.
[13] A. Kafle, S. Lu, R. Silwal, W. Zhu. *A Review on Material Dynamics in Cold Spray Additive Manufacturing: Bonding, Stress, and Structural Evolution in Metals*. **Metals**, **15**, 2025, 187.
[14] W. Li, F. Huang, S. Liu, H. Wu, X. Chu, Y. Xie, C. Deng, C. Verdy, S. Deng. *Hybrid cold spray additive-subtractive manufacturing with adaptive path planning for autonomous repair of complex geometrical defects*. **Journal of Manufacturing Processes**, **152**, 2025, 1037–1050.
[15] M. Galati. *Electron beam melting process: a general overview*. **Handbooks in Advanced Manufacturing: Additive Manufacturing**, 2021, 277–301.
[16] C. Körner. *Additive manufacturing of metallic components by selective electron beam melting — a review*. **International Materials Reviews**, **61(5)**, 2016, 361–377.
[17] T.C. Dzogbewu, D. de Beer. *Powder Bed Fusion of Multimaterials*. **Journal of Manufacturing and Materials Processing**, **7**, 2023, 15.
[18] C. Burkhardt, S. Henkel, H. Biermann, A. Weidner. *Influence of alloy composition on microstructural and mechanical properties of lattice structures made of high-alloyed austenitic TRIP/TWIP steel produced by selective electron beam melting*. **Materials Science and Engineering A**, **930**, 2025, 148073.
[19] C.Y. Kong, R.C. Soar, P.M. Dickens. *Optimum process parameters for ultrasonic consolidation of 3003 aluminium*. **Journal of Materials Processing Technology**, **146(2)**, 2004, 181–187.
[20] ASTM. *F2792-12A Standard Terminology for Additive Manufacturing Technologies*. ASTM International, 2012.
[21] W. Li, H. Assadi, F. Gaertner, S. Yin. *A Review of Advanced Composite and Nanostructured Coatings by Solid-State Cold Spraying Process*. **Critical Reviews in Solid State**, **44(2)**, 2019, 109–156.
[22] S. Yin, P. Cavaliere, B. Aldwell, R. Jenkins, H. Liao, W. Li, R. Lupoi. *Cold spray additive manufacturing and repair: Fundamentals and applications*. **Additive Manufacturing**, **21**, 2018, 628–650.
[23] H. Wang, P. Li, W. Guo, G. Ma, H. Wang. *Copper-Based Composite Coatings by Solid-State Cold Spray Deposition: A Review*. **Coatings**, **13**, 2023, 479.
[24] H. Assadi, F. Gärtner, T. Stoltenhoff, H. Kreye. *Bonding mechanism in cold gas spraying*. **Acta Materialia**, **51**, 2003, 4379–4394.
[25] Y. Ichikawa, R. Tokoro, M. Tanno, K. Ogawa. *Elucidation of cold-spray deposition mechanism by auger electron spectroscopic evaluation of bonding interface oxide film*. **Acta Materialia**, **164**, 2019, 39–49.
[26] P.K. Gokuldoss, S. Kolla, J. Eckert. *Additive Manufacturing Processes: Selective Laser Melting, Electron Beam Melting and Binder Jetting—Selection Guidelines*. **Materials**, **10**, 2017, 672.
[27] L.-C. Zhang, Y. Liu, S. Li, Y. Hao. *Additive Manufacturing of Titanium Alloys by Electron Beam Melting: A Review*. **Advanced Engineering Materials**, **20**, 2018, 1700842.
[28] S. Biamino, A. Penna, U. Ackelid, S. Sabbadini, O. Tassa, P. Fino, M. Pavese, P. Gennaro, C. Badini. *Electron beam melting of Ti–48Al–2Cr–2Nb alloy: Microstructure and mechanical properties investigation*. **Intermetallics**, **19(6)**, 2011, 776–781.
[29] C.A. Terrazas, S.M. Gaytan, E. Rodriguez. *Multi-material metallic structure fabrication using electron beam melting*. **International Journal of Advanced Manufacturing Technology**, **71**, 2014, 33–45.
[30] D. Li. *A review of microstructure evolution during ultrasonic additive manufacturing*. **International Journal of Advanced Manufacturing Technology**, **113**, 2021, 1–19.
[31] A.A. Mukhametgalina, M.A. Murzinova, A.A. Nazarov. *Microstructure of a titanium sample produced by ultrasonic consolidation*. **Letters on Materials**, **12(2)**, 2022, 153–157.
[32] M.R. Sriraman, S.S. Babu, M. Short. *Bonding characteristics during very high power ultrasonic additive manufacturing of copper*. **Scripta Materialia**, **62(8)**, 2010, 560–563.

[33] E.R. Shayakhmetova, M.A. Murzinova, V.S. Zadorozhniy, A.A. Nazarov. *Microstructure of Joints Processed by Ultrasonic Consolidation of Nickel Sheets*. **Metals**, **12**, 2022, 1865.
[34] Y. Wang, Q. Yang, X. Liu, Y. Liu, B. Liu, R.D.K. Misra, H. Xu, P. Bai. *Microstructure and mechanical properties of amorphous strip/aluminum laminated composites fabricated by ultrasonic additive consolidation*. **Materials Science and Engineering A**, **749**, 2019, 74–78.
[35] S. Yin, M. Meyer, W. Li, H. Liao, R. Lupoi. *Gas flow, particle acceleration, and heat transfer in cold spray: a review*. **Journal of Thermal Spray Technology**, **25**, 2016, 1–23.
[36] J.O. Obielodan, A. Ceylan, L.E. Murr, B.E. Stucker. *Multi-material bonding in ultrasonic consolidation*. **Rapid Prototyping Journal**, **16(3)**, 2010, 180–188.
[37] N. Sridharan, P. Wolcott, M. Dapino, S.S. Babu. *Microstructure and texture evolution in aluminum and commercially pure titanium dissimilar welds fabricated using ultrasonic additive manufacturing*. **Scripta Materialia**, **117**, 2016, 1–5.
[38] J. Bo, R. Xueping, H. Yujie, H. Hongliang, W. Yaoqi. *Mechanical properties and bonding mechanism of Ti/Al-laminated composites fabricated by ultrasonic consolidation*. **ACM**, **30**, 2021.
[39] Y. Zhou, Z. Wang, J. Zhao, F. Jiang. *Effect of ultrasonic amplitude on interfacial characteristics and mechanical properties of Ti/Al laminated metal composites fabricated by ultrasonic additive manufacturing*. **Additive Manufacturing**, **74**, 2023, 103725.
[40] Y. Cheng, Z. Wu, X. He, Y. Zhou, C. Xu, Z. Niu, F. Jiang, C. Xu, Z. Wang. *In-situ study of tensile behavior of Ti/Al laminated metal composites fabricated via ultrasonic additive manufacturing*. **Composites Communications**, **51**, 2024, 102095.
[41] M. de Leon, H.-S. Shin. *Review of advancements in aluminum and copper ultrasonic welding in electric vehicles and superconductor applications*. **Journal of Materials Processing Technology**, **307**, 2022, 117691.
[42] X. Wu, T. Liu, W. Cai. *Microstructure, welding mechanism, and failure of Al/Cu ultrasonic welds*. **Journal of Manufacturing Processes**, **20(1)**, 2015, 321–331.
[43] H.T. Fujii, H. Endo, Y.S. Sato, H. Kokawa. *Interfacial microstructure evolution and weld formation during ultrasonic welding of Al alloy to Cu*. **Materials Characterization**, **139**, 2018, 233–240.
[44] W. Zhao, B. Liu, Y. Wang, Y. Chen, L. Feng. *Properties of ultrasonically consolidated Al/Cu laminated composites and the attenuation effect of shock waves*. **Journal of Materials Research and Technology**, **29**, 2024, 3866–3878.
[45] Y. Yang, G.D. Ram, B.E. Stucker. *Bond formation and fiber embedment during ultrasonic consolidation*. **Journal of Materials Processing Technology**, **209(10)**, 2009, 4915–4924.
[46] G.D. Janaki Ram, C. Robinson, Y. Yang, B. Stucker. *Use of ultrasonic consolidation for fabrication of multi-material structures*. **Rapid Prototyping Journal**, **13**, 2007, 226–235.
[47] D. Erdeniz, T. Ando. *Fabrication of micro/nano structured aluminum–nickel energetic composites*. **International Journal of Materials Research**, **104**, 2012, 386–391.
[48] T. Hussain, D.G. McCartney, P.H. Shipway. *Bonding between aluminium and copper in cold spraying: story of asymmetry*. **Materials Science and Technology**, **28(12)**, 2012, 1371–1378.
[49] T. Hussain, D.G. McCartney, P.H. Shipway. *Bonding mechanisms in cold spraying: The contributions of metallurgical and mechanical components*. **Journal of Thermal Spray Technology**, **18**, 2009, 364–379.
[50] P.C. King, G. Bae, S.H. Zahiri. *An Experimental and Finite Element Study of Cold Spray Copper Impact onto Two Aluminum Substrates*. **Journal of Thermal Spray Technology**, **19**, 2010, 620–634.
[51] A.M. Ralls, M. Daroonparvar, M. John, S. Sikdar, P.L. Menezes. *Solid-State Cold Spray Additive Manufacturing of Ni-Based Superalloys: Processing–Microstructure–Property Relationships*. **Materials**, **16**, 2023, 2765.

[52] X.-T. Luo, M.-L. Yao, N. Ma, M. Takahashi, C.-J. Li. *Deposition behavior, microstructure and mechanical properties of an in-situ micro-forging assisted cold spray enabled additively manufactured Inconel 718 alloy*. **Materials and Design**, **155**, 2018, 384–405.
[53] A. Chaudhuri, Y. Raghupathy, D. Srinivasan, S. Suwas, C. Srivastava. *Microstructural evolution of cold-sprayed Inconel 625 superalloy coatings on low alloy steel substrate*. **Acta Materialia**, **129**, 2017, 11–25.
[54] W. Wong, E. Irissou, P. Vo, M. Sone, F. Bernier, J.G. Legoux, S. Yue. *Cold spray forming of Inconel 718*. **Journal of Thermal Spray Technology**, **22**, 2013, 413–421.
[55] K. Wu, W. Sun, A. Wei-Yee Tan, I. Marinescu, E. Liu, W. Zhou. *Microstructure, tribological and mechanical properties of cold sprayed Inconel 625 coatings*. **Surface and Coatings Technology**, **424**, 2021, 127660.
[56] D. Levasseur, S. Yue, M. Brochu. *Pressureless sintering of cold sprayed Inconel 718 deposit*. **Materials Science and Engineering A**, **556**, 2012, 343–350.
[57] A. Silvello, P. Cavaliere, A. Rizzo. *Fatigue Bending Behavior of Cold-Sprayed Nickel-Based Superalloy Coatings*. **Journal of Thermal Spray Technology**, **28**, 2019, 930–938.
[58] T. Hussain, D.G. McCartney, P.H. Shipway. *Impact phenomena in cold-spraying of titanium onto various ferrous alloys*. **Surface and Coatings Technology**, **205**, 2011, 5021–5027.
[59] G. Bae, S. Kumar, S. Yoon, K. Kang, H. Na, H.-J. Kim, C. Lee. *Bonding features and associated mechanisms in kinetic sprayed titanium coatings*. **Acta Materialia**, **57(19)**, 2009, 5654–5666.
[60] C.K.S. Moy, J. Cairney, G. Ranzi, M. Jahedi, S.P. Ringer. *Microstructure and composition of cold gas-dynamic spray Ti powder deposited on Al 6063 substrate*. **Surface and Coatings Technology**, **204(23)**, 2010, 3739–3749.
[61] H.R. Wang, B.R. Hou, J. Wang. *Effect of process conditions on microstructure and corrosion resistance of cold-sprayed Ti coatings*. **Journal of Thermal Spray Technology**, **17**, 2008, 736–741.
[62] S. Gulizia, A. Clayton, A. Trentin, S. Vezzù, S. Rech, P. King, M. Jahedi, M. Guagliano. *Microstructure and Mechanical Properties of Cold Spray Titanium Coatings*. **International Thermal Spray Conference**, 2010.
[63] W. Wong, A. Rezaeian, E. Irissou, J.G. Legoux, S. Yue. *Cold spray characteristics of commercially pure Ti and Ti-6Al-4V*. **Advanced Materials Research**, **89–91**, 2010, 639–644.
[64] A. Zykova, A. Vorontsov, A. Nikolaeva, A. Chumaevskii, K. Kalashnikov, D. Gurianov, N. Savchenko, S. Nikonov, E. Kolubaev. *Structural design and performance evaluation of Ti6Al4V/5%Cu produced by electron-beam additive technology with simultaneous double-wire feeding*. **Materials Letters**, **312**, 2022, 131586.
[65] C. Guo, W. Ge, F. Lin. *Dual-Material Electron Beam Selective Melting: Hardware Development and Validation Studies*. **Engineering**, **1(1)**, 2015, 124–130.
[66] A. Hinojos, J. Mireles, A. Reichardt, P. Frigola, P. Hosemann, L.E. Murr, R.B. Wicker. *Joining of Inconel 718 and 316 Stainless Steel using electron beam melting additive manufacturing technology*. **Materials and Design**, **94**, 2016, 17–27.
[67] G. Zhu, L. Wang, B. Wang, B. Li, J. Zhao, B. Ding, R. Cui, B. Jiang, C. Zhao, Y. Su, R. Chen, Y. Su, J. Guo. *Multi-materials additive manufacturing of Ti64/Cu/316L by electron beam freeform fabrication*. **Journal of Materials Research and Technology**, **26**, 2023, 8388–8405.
[68] W. Wenjun, G. Chao, L. Feng. *Microstructures of components synthesized via electron beam selective melting using blended pre-alloyed powders of Ti6Al4V and Ti45Al7Nb*. **Rare Metal Materials and Engineering**, **44(11)**, 2015, 2623–2627.

Received: June 06, 2025
Accepted: November 21, 2025